7. Vacuum System

7.1 Introduction

Beam lifetime and beam stability are of major importance to any synchrotron; the interaction of the stored particles with the residual gas molecules leads to particles losses caused by scattering processes. Because of this a detailed design of the vacuum system is essential. Thus, the vacuum system design, requirements and the calculations for SESAME will be discussed and summarized here.

In general the design will be based on ANKA, SLS and CLS vacuum system designs.

7.2 SESAME Parameters

General characteristics of the machine are tabulated in Table (7.1) [1]:

Table 7.1: SESAME main parameters

Beam Energy (GeV)	2
Beam Current (mA)	400
Horizontal Emittance (nm)	16.960
Number of Straights	16 of which: 8 Wigglers 1 Injection 2 RF Cavities 5 Undulators
Circumference (m)	120.0
Dipole Bending radius (m)	4.942
Dipole magnet length (m)	1.941
Dipole Magnetic Field (T)	1.350

These Parameters are the most important from vacuum point of view, others like photon flux, photodesorption yield, average pressure…etc will be calculated later on.

7.3 Requirements

Basic requirements common to most storage ring UHV systems are:

- Beam lifetime more than 10 hours
- Smooth chamber to minimize electromagnetic fields induced by the beam
- Sufficient cooling, to dissipate the heat load associated with synchrotron radiation
- Good and sufficient monitoring; achieving the pressure is as much important as evaluating that pressure correctly
- Separation of the sectors by pneumatic valves
- Reasonable cost
- Flexible system for improvements and upgrading
- Reliable system

7.4 Materials for Vacuum Chamber

7.4.1 General

In general, synchrotron light source vacuum chambers are fabricated from stainless steel, aluminium or copper. However copper is used internally for photon stop or radiation absorbers, where high heat loads have to be dissipated. Titanium, Beryllium, ceramics and Nickel alloys have also been used for special purposes.

Many factors need to be taken into account to select the suitable material to be used in the vacuum system; vacuum performance, mechanical strength (stability, hardness), thermal conductivity, magnetic permeability, surface resistivity, materials vapour pressure, how easy the material is for fabrication, joining and cleaning.

Concerning vacuum performance; the main vacuum property to be discussed is the photon desorption yield and its reduction with beam dose, see Figure (7.1) [2].

(a) Stainless Steel   **(b) Aluminium**   **(c) Copper**
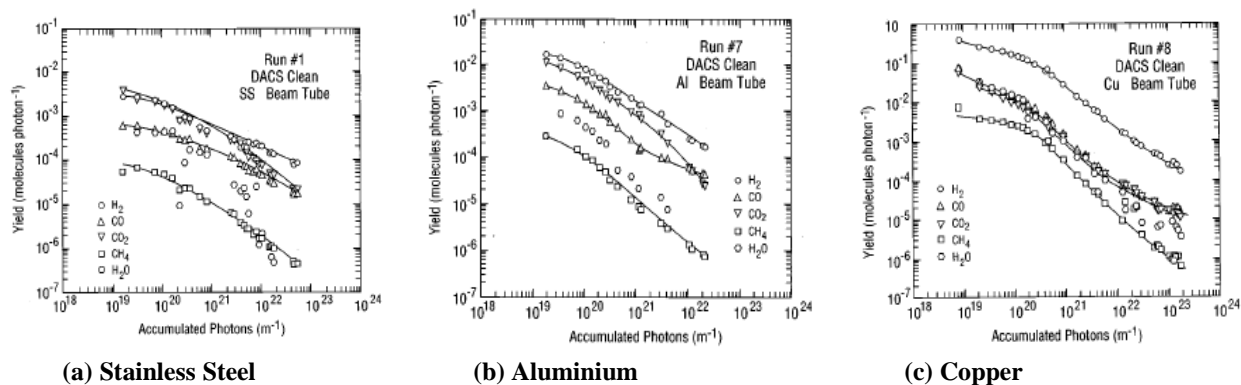
Figure 7.1: Photon stimulation desorption yield reduction with accumulated beam dose for (a) stainless steel, (b) aluminium and (c) copper

One can notice that almost all behave similarly, however copper and aluminium show higher photodesorption initially than stainless steel. It has been shown by experiments that a surface which has been vented after being 'scrubbed' by the beam will not give yields as high as a surface which has not been 'scrubbed', however, aluminium is the worst in comparison to stainless steel and copper.

Aluminium has good properties such as: it is easy for manufacturing by extrusion especially for long beam tubes and complex chambers, also it has good thermal conductivity and it is completely non magnetic. However aluminium has several disadvantages such as it has weak mechanical properties, higher desorption yield and it is difficult for joining.

Copper (OFHC copper) is used for UHV applications; it has good thermal conductivity but it has higher desorption yield compared to stainless steel. Also its production process is more complicated and expensive in comparison to aluminium (if copper is used for vacuum vessels with an antechamber, the chambers need to be extruded separately from the antechamber and welded together afterwards) [3].

Stainless steel (316LN alloy) is usually used for UHV applications. It has good mechanical strength, is easy to weld, has high hardness and low outgassing rates. It also has a low magnetic permeability so it can be used within magnets. The thermal conductivity of stainless steel is very poor in comparison to copper, therefore to transport high heat loads (e.g. in absorbers) copper plates need to be used. Also the value of electrical conductivity is very low (low eddy currents, resistive wall effect) [4] for the stainless steel.

Stainless steel can be baked out up to (350°C) to remove water and fired (up to 900°C) to reduce H_2.

Stainless steel seems to be a suitable material for SESAME vacuum chambers because of its properties, however OFHC copper should be used for the absorbers.

There are two more arguments for choosing stainless steel as the material for the vacuum chamber:

- One should use a material, which can be handled by the accelerator laboratory and there exist expertise to deal with them.

76

- The vacuum system should be build by the industry. Within the industry most experiences are available with stainless steel.

All these arguments are in favor of stainless steel as the suitable material for the vacuum chamber.

7.4.2 Vacuum Chamber Design

The design of the vacuum chamber is not an easy task; many factors must be taken into consideration to have the right size of the vacuum chamber; Touschek scattering, gas scattering, closed-orbit errors, injection requirements and momentum acceptance. Taking these into account will give the beam stay clear which therefore will give the minimum required aperture. The actual machine aperture may lie out of this because of RF or engineering requirements.

There mainly are two principles for the vacuum chamber design: 1) a straight with full antechamber design (3rd generation synchrotron light sources like SLS and CLS) 2) a vacuum chamber in which the antechamber is only in the bending and the first following focusing magnet and a single chamber vacuum vessel with a distributed photon absorber in the rest of the ring (2nd generation synchrotron light sources like ANKA).

Slit opening height between the vacuum chamber and the antechamber in the dipole must be decided carefully to prevent the high local thermal stress, which can be achieved by increasing the height of the slit or water-cooled copper shield along the vacuum chamber between the antechamber

The introduction of the electrode of the BPM into the vacuum system can be done by one of the following ways:

a) Welding it directly to the BPM blocks
b) Using a separate flange to hold the electrodes, which is connected to the BPM blocks

The BPM must be bolted rigidly to the magnet girders. To get rid of misreading of the BPM two options are available:

1) The BPM electrode can be connected to bellows to allow movement of the vacuum chambers.
2) The movements of the vacuum chamber are detected by optical sensors and can be compensated for when reading the BPM [4], [5].

In order to avoid the extra cost of having a separate flange for the BPM one solution is to weld the BPM electrode directly to the BPM blocks and bolt it to the girders and connect it to the bellows to get rid of the misreading.

Manufacturing should be done in such a way to eliminate trapped volumes (e.g. due to poor welding) to get better vacuum performance since these volumes will increase the pump down time due to virtual leaks appearing [6].

All components need to be cleaned properly. Cleaning procedures must guarantee that all components will be suitable for UHV. Cleaning will reduce the evolution of the gases from the surfaces, the source of these gases can be oils, greases, fluxes, fingerprints…etc. Cleaning should be suitable for the material type and should not leave any deposits behind [6].

7.5 Calculations

Basic calculations for any vacuum system design need to be carried out in such a way to achieve important values for the system; such as photon flux, pressure profile, power dissipation…etc.

The pressure profile may be used for the optimization of the vacuum system. The profile gives the best location for the pumps and type of pumps (lumped or distributed) needed to be installed. The pressure profile can also give an indication of the location of the absorbers and the required number to get the lowest average dynamic pressure.

The storage ring will be divided into 8 cells and each cell will contain one straight and two dipole bending magnets; see Figure (7.2) and the discussion in section 5.1. Figure (7.2) shows the unit cell with the pumps distributed along the chamber. This layout, which has been used for the evaluation of the pressure profile, is simply based on the space available between the magnets to put in the pumping ports. A further decision has to be made on the location of the pumping ports shown in Figure (7.2). One possibility is to put the pumping ports underneath the vacuum chamber; this will allow the designer to have a wider pumping port without limiting the available space, therefore, decreasing the conductance limitation of the system.
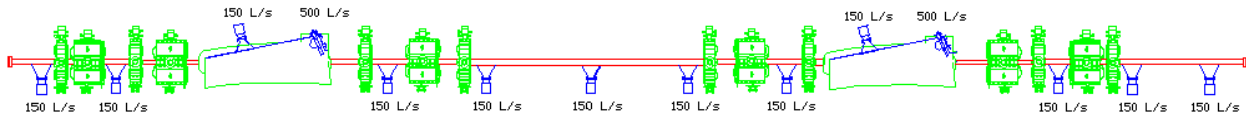
Figure 7.2: SESAME cell (1/8 of the storage Ring) and basic layout for the pumps distribution

Calculations have been carried out for unbaked stainless steel vacuum chamber for CO (mass 28) at 293K. The vacuum and antechamber dimensions and profiles are described in sections 5.3, 5.4 and 5.5. The dipole vacuum chamber design is based on the one used for ANKA.

Evaluation of the pressure profile along the storage ring can be done in several ways; one possible method is the Monte-Carlo simulation, which gives accurate results but exact dimensions of the vacuum chamber should already be known. Since at this stage of the project there are no detailed drawings of the vacuum chamber, it is not possible to use the Monte-Carlo simulation. Instead, the pressure profile will be calculated analytically.

The calculations will be performed based on the gas dynamic balance equation inside a vacuum chamber [7], as shown in Equation (7.1):

$$V\frac{dn}{dt} = q - cn + u\frac{d^2 n}{dL^2} \qquad (7.1)$$

Where: V is vacuum chamber volume,
           n is the gas density,
           q the gas desorption flux from both thermal desorption and photo stimulated desorption

$$q = \eta_t F + \eta_\gamma \Gamma \qquad (7.2)$$

Where: F is surface area,
           Γ is the photon flux,
           η_t , η_γ are the thermal and photo stimulation desorption yields,
           L is the longitudinal axis of the vacuum chamber.

A detailed discussion along with the solution of this equation is presented in reference [7].

Detailed calculations[1] for SESAME (under the previous conditions of the design) have been carried out using the Mathcad program, however this report will include only the results achieved for SESAME.

7.5.1 Photon Flux from the Dipoles

The radiation from the dipoles will find its way into 3 possible places: 1) to the crotch absorber 2) to the beam line front ends 3) It irradiates the walls of the vacuum chamber.

Equation (7.3) shows that the total photon flux for SESAME with a beam energy (E) of 2GeV and a beam current (I) of 400mA is 6.43×10^{20} photons/s.

---

[1] - Calculations have been carried out with the help of ASTeC Vacuum Science Group/ Daresbury Laboratories.

$$\Gamma_{tot} = 8 \times 10^{20} E.I \qquad\qquad (7.3)$$

Each dipole radiates 4.021×10^{19} photons/s at an angle of 393 mrad (22.5°). For the calculations however the assumption is that only 300 mrad of this angle hits the crotch absorber.

Equation (7.4) has been used in the evaluation of the photon flux distribution per unit lenght of the vacuum chamber based on the geometry of the vacuum chamber.

$$\Gamma(a, L, L1) = \Gamma_{rad} \cdot \frac{(R_d + a)\sqrt{(L^2 + 2.R_d.a^2)} - LR_d}{[(R_d + a)^2 + L^2]\sqrt{L^2 + 2.R_d.a + a^2}} \qquad\qquad (7.4)$$

Where: $\Gamma(a,L,L1)$ is the photon flux in (photons/m.s) for L, the distance from the dipole,
          a is the long radius of the elliptical vacuum chamber,
          Γ_{rad} is the angular photon flux (photons/rad.s), $\Gamma_{rad=}1.28x10^{20}.E.I,$
          R_d is the bending radius,
          $L1$ is the length of the straight.

This formula gives the photon flux distribution from the dipoles taking into account the angle at which the photon hits the chamber walls (incident angle).

Figure (7.3) shows the photon flux (photons/m.s), which varies from $2x10^{19}$ all over the dipole to $1x10^{17}$ photons/m.s at the end of the straight section.
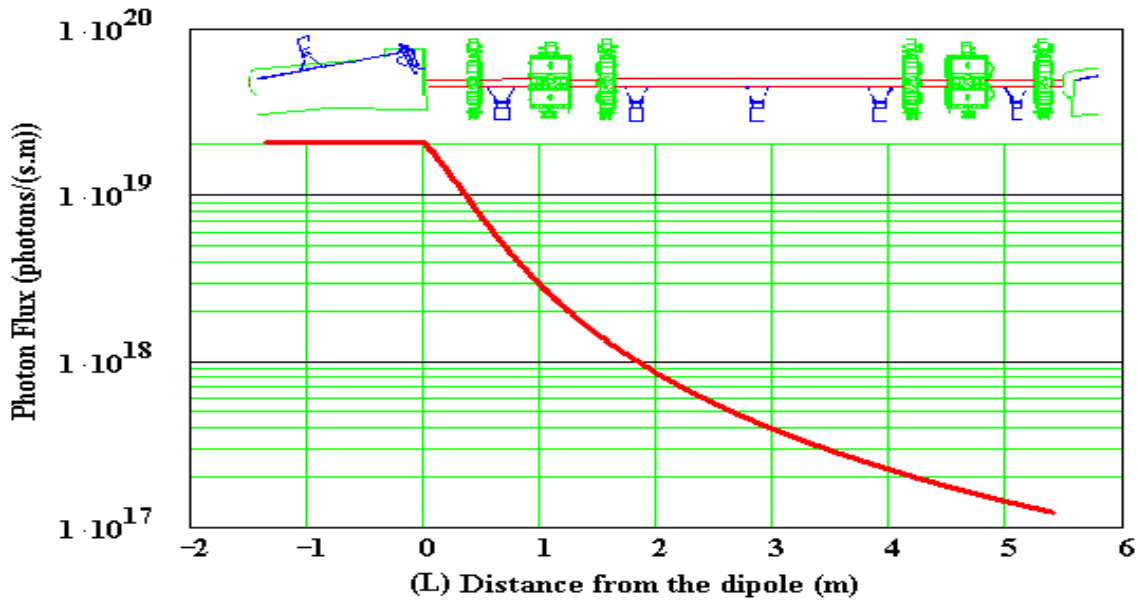
Figure 7.3: Photon flux distribution per meter of the vacuum chamber

7.5.2 Photon Stimulated Desorption (PSD)

The PSD yield η(molecules/photons) for the vacuum chamber decreases with photon dose (D=Γ.time) proportionally to $D^{-\alpha}$. Figure (7.4) shows the PSD yield reduction versus the dose for the baked and unbaked vacuum chambers. The difference between the two curves is significant at low values of photon dose. At high doses, however, the yields are more or less similar. The calculations are based on the unbaked system since it gives higher yield values.

79
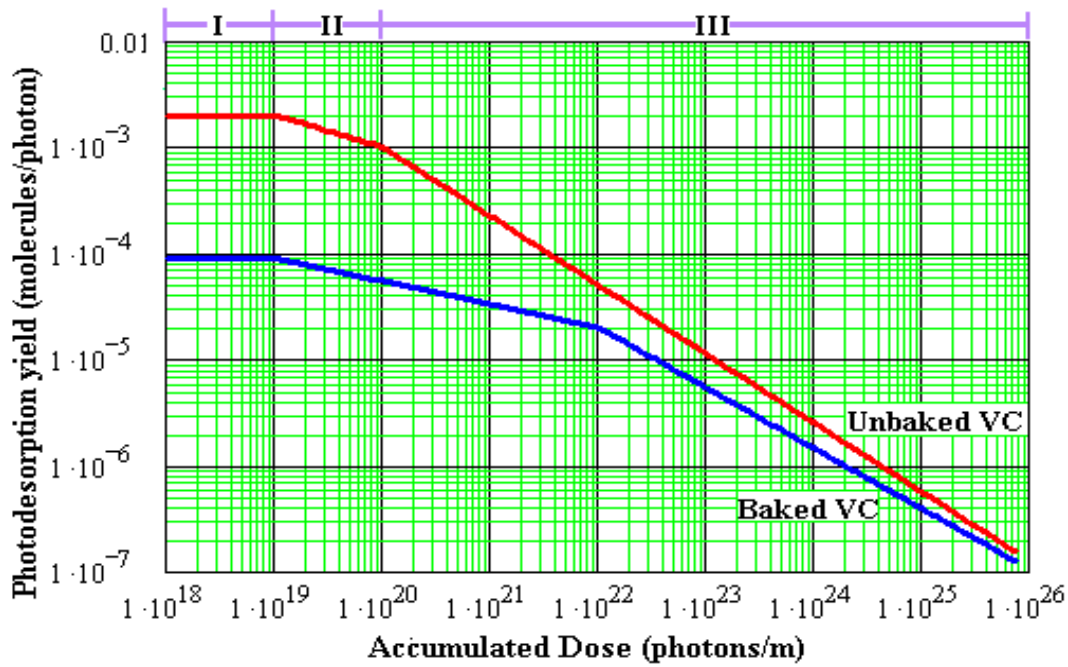
Figure 7.4: PSD yield for CO for unbaked and baked vacuum chambers
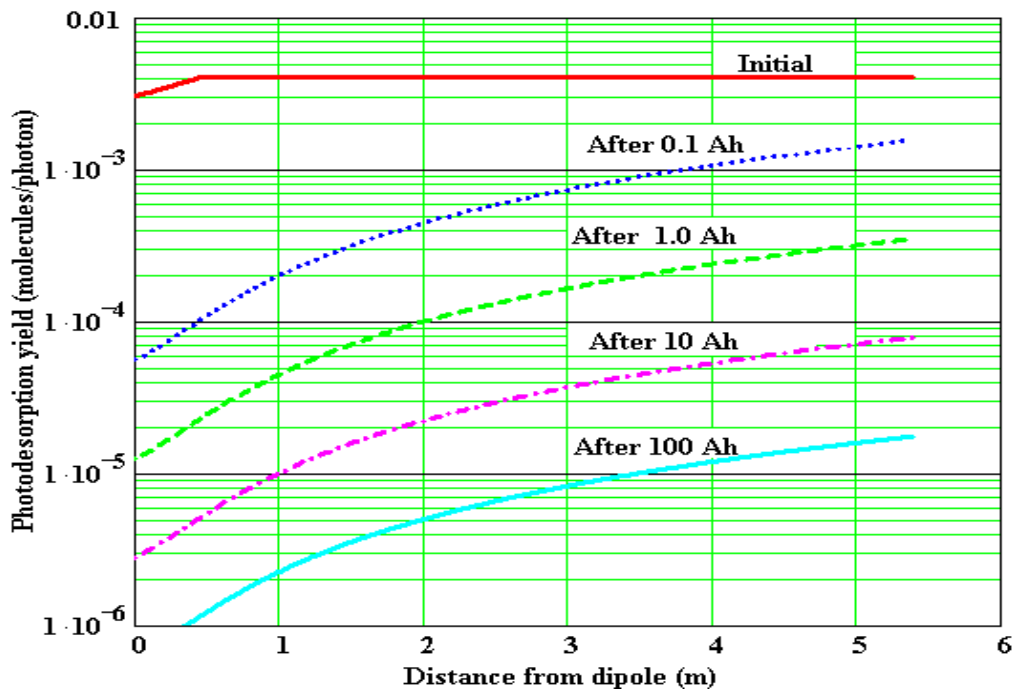
Figure 7.5: Photodesorption yield for the straight section per unit length as a function of the beam dose

The curve has been divided into 3 ranges according to the slope of the curve. Equation (7.4) shows the ranges for each slope which have been used for the calculations.

$$\eta = \begin{cases} 0.004 & D \le 10^{19} & \text{(I)} \\ 0.004(\dfrac{10^{19}}{D})^{0.3} & 10^{19} \langle D \langle 10^{20} & \text{(II)} \\ 2\times 10^{-3}(\dfrac{10^{20}}{D})^{0.65} & \text{otherwise} & \text{(III)} \end{cases} \qquad (7.5)$$

7.5.3 Photodesorption Along the Straight

The desorption flux (molecules/s) can be simply achieved by multiplying the yield by the photon flux. Since the photon flux depends on the distance from the dipole, the values of the photodesorption yield and flux will also vary with distance from the dipole. Figures (7.5) and (7.6) show the desorption yield and the flux as a function of distance from the dipole for different beam doses.
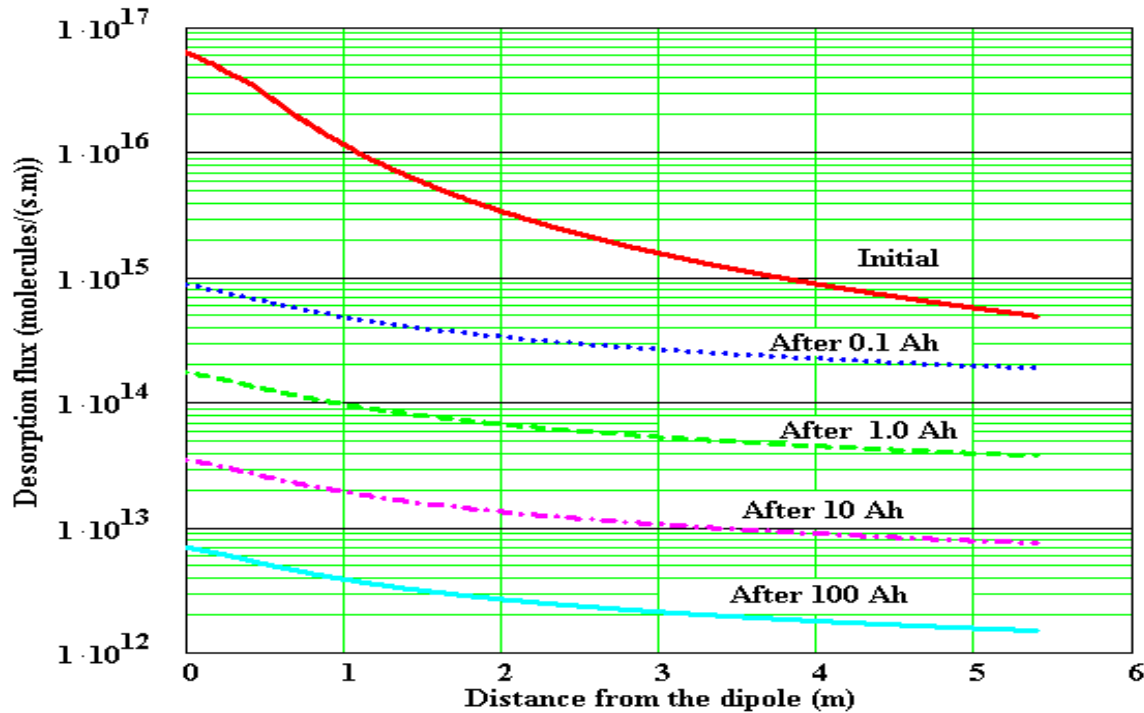
Figure 7.6: Desorption flux for the straight section per unit length and as a function of the beam dose

7.5.4 Thermal Desorption

The thermal desorption have been calculated taking the following parts into consideration: vacuum chamber, antechamber, the front ends (assuming the front ends length is 2.5m) and the pumping ports (assuming the pumping ports are 0.5m long), the thermal outgassing rate of 10^{-11} mbar.lt/(sec.cm^2).

7.5.5 Pressure Profile

For the evaluation of the pressure profile, the vacuum chamber has been divided into parts; each defined upon its function (pumping part or not…) and location. This arrangement allows definition of the parts and the distribution be changed more easily. Table (7.2) shows one of the databases for the vacuum chamber of SESAME with one absorber (200 mm width) and pumps along the chamber with 250 mm pumping ports (pumping port for the dipole pump is of 300 mm

width). l is the length of the part, L is the accumulated length from the beginning of the achromat, x_{ap} and y_{ap} are the dimensions of the vacuum chamber.

Table 7.2: The vacuum chamber divided into sections for the calculation purposes

ACHROMAT VACUUM CHAMBER ELEMENTS							
l (mm)	L (mm)	X (m)	Y (m)	Pumping	Photons	Antechamber (m)	Element
250	250	0.035	0.015	Lumped pump	Distributed flux	0	Achromat end pump
640	890	0.035	0.015	No pump	Distributed flux	0	VC
250	1140	0.035	0.015	Lumped pump	Distributed flux	0	Pump
570	1710	0.035	0.015	No pump	Distributed flux	0	VC
500	2210	0.035	0.015	No pump	Photons in the Dipole VC.	0.08094	Dipole VC
300	2510	0.035	0.015	Lumped pump	Photons in the Dipole VC.	0.11181	Pump
891	3401	0.035	0.015	No pump	Photons in the Dipole VC.	0.22059	Dipole VC
250	3651	0.035	0.015	Lumped pump + absorber	Photons in the Dipole VC.	0.39540	Absorber + Pump
350	4001	0.035	0.015	No pump	Distributed flux	0	VC
250	4251	0.035	0.015	Lumped pump	Distributed flux	0	Pump
640	4891	0.035	0.015	No pump	Distributed flux	0	VC
250	5141	0.035	0.015	Lumped pump	Distributed flux	0	Pump
1084	6225	0.035	0.015	No pump	Distributed flux	0	VC
250	6475	0.035	0.015	Lumped pump	Distributed flux	0	Pump
1084	7559	0.035	0.015	No pump	Distributed flux	0	VC
250	7809	0.035	0.015	Lumped pump	Distributed flux	0	Pump
640	8449	0.035	0.015	No pump	Distributed flux	0	VC
250	8699	0.035	0.015	Lumped pump	Distributed flux	0	Pump
350	9049	0.035	0.015	No pump	Distributed flux	0	VC
500	9549	0.035	0.015	No pump	Photons in the Dipole VC.	0.08094	Dipole VC
300	9849	0.035	0.015	Lumped pump	Photons in the Dipole VC.	0.11181	Pump
891	10740	0.035	0.015	No pump	Photons in the Dipole VC.	0.22059	VC
250	10990	0.035	0.015	Lumped pump + absorber	Photons in the Dipole VC.	0.39540	Absorber + Pump
570	11560	0.035	0.015	No pump	Distributed flux	0	VC
250	11810	0.035	0.015	Lumped pump	Distributed flux	0	Pump
640	12450	0.035	0.015	No pump	Distributed flux	0	VC
250	12700	0.035	0.015	Lumped pump	Distributed flux	0	Pump
1025	13725	0.035	0.015	No pump	Distributed flux	0	VC
250	13975	0.035	0.015	Lumped pump	Distributed flux	0	Pump
1025	15000	0.035	0.015	No pump	Distributed flux	0	VC
250	15250	0.035	0.015	Lumped pump	Distributed flux	0	Pump

For this data and with 500l/s effective absorber pumping speed (assuming an efficiency of 50% at 10^{-9} mbar) and 150l/s nominal pumping speed for the pumps along the achromat (assume 100l/s effective pumping speed), an average pressure of 1.233×10^{-9} mbar has been achieved.

Figure (7.7) shows the base pressure profile (due to thermal desorption / without SR beam) and the dynamic pressure (due to both the thermal and the photo stimulated desorption / with SR beam).
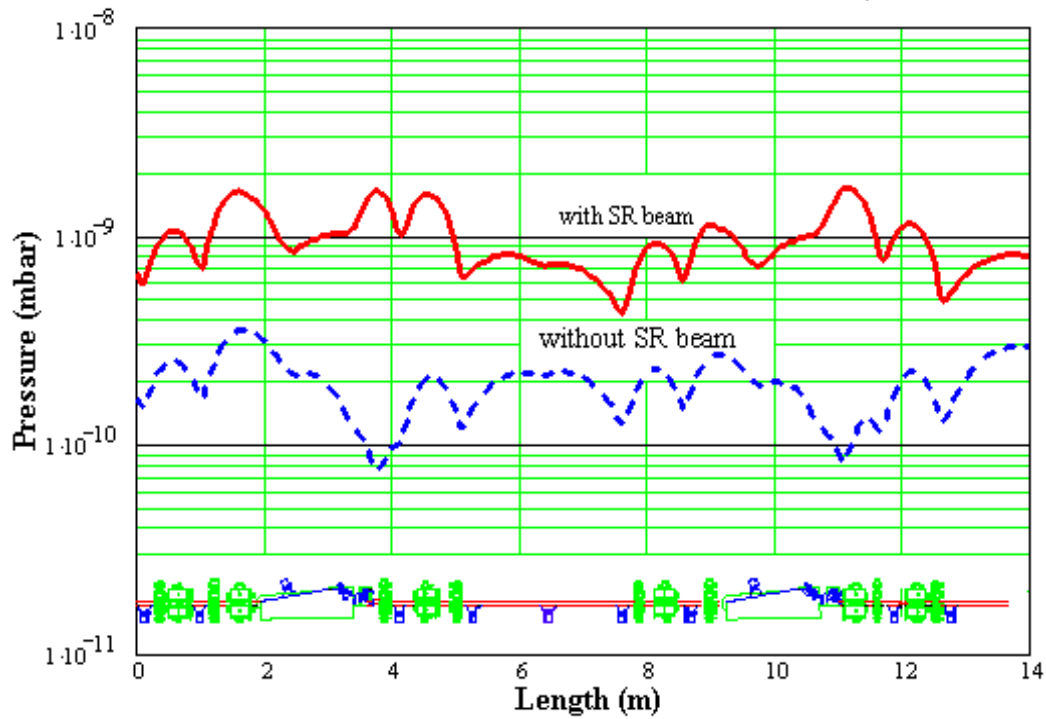
Figure 7.7: Pressure profile for one cell of the vacuum chamber (1/8 of the storage ring), $P_{av,T} = 9.35 \times 10^{-10}$ mbar, $P_{av,PSD} = 2.97 \times 10^{-10}$ mbar, $P_{av} = 1.233 \times 10^{-9}$ mbar

This is the profile that will be achieved from the design proposed in this stage of the project. The following changes however could give lower values for the average pressure:

1) Increasing the pumping speed for the pumps close to the absorber to a value of 1000 l/s will reduce the pressure to a value of 1.164×10^{-9} mbar.

2) Increasing the pumping speed for the pumps along the vacuum chamber from 150 l/s to 200 l/s (about 150 l/s effective pumping speed) will decrease the average pressure to 9.66×10^{-10} mbar.

3) Changing the design to have two absorbers with 200 mm width and 750 l/s pumping speed, and pumps along the unit cell with 150 mm width and 150 l/s pumping speed results an average dynamic pressure of 9.43×10^{-10} mbar as shown in Figure (7.8).
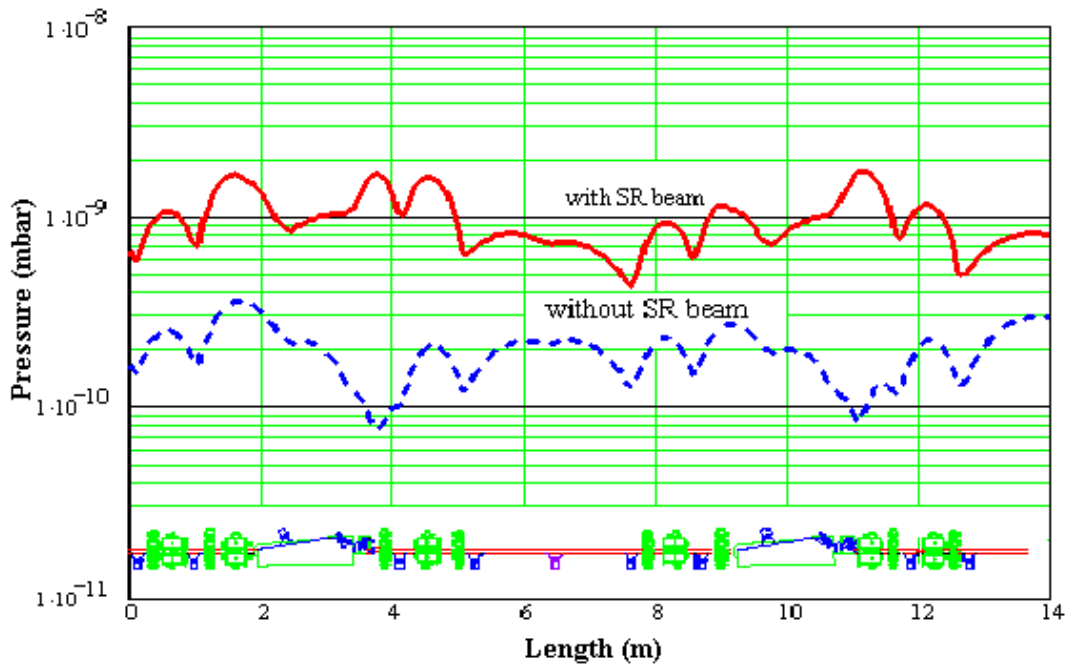
Figure 7.8: The pressure profile for SESAME cell with two absorbers of 200mm width and 750l/s pumping speed, pumps along the achromat with 150mm width and 150l/s pumping speed, $P_{av} = 9.43 \times 10^{-10}$ mbar

4) Increasing the pumping speed for the pump near the absorber to 1000 l/s for the case (3) will decrease the average pressure down to 8.79×10^{-10} mbar.

5) Adding a third absorber to the case (3) in the straight section and before the third sextupole will increase the average pressure to 1.107×10^{-9} mbar, because it will increase the base pressure due to the area increase (the antechamber). Figure (7.9) shows the pressure profile for this case.
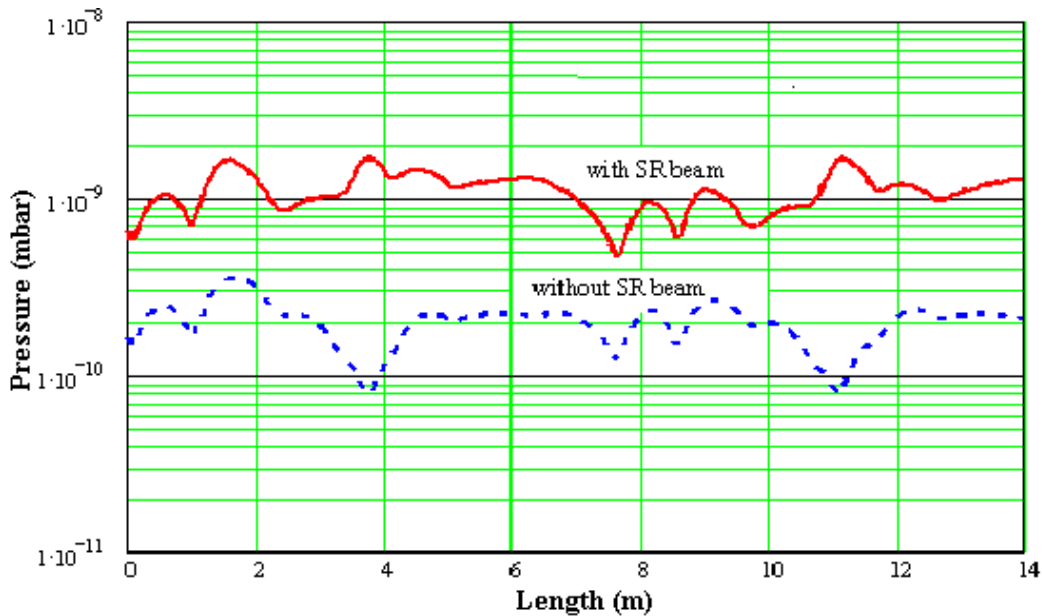
Figure 7.9: The pressure profile for the SESAME cell with 3 absorbers (200 mm and 750 l/s) and pumps along the cell (150 mm and 150 l/s)

84

The increasing of the pumping speed may decrease the dynamic pressure of the system however. Due to the conductance limitation, the improvements would reach to a point that further increase would decrease the pressure slightly. Figure (7.10) shows the average pressure variation with the absorber pumps pumping speed of 100 l/s and 150 l/s for the pumps distributed along the chamber. Figure (7.11) shows the average pressure variation with different pumping speeds (1000 l/s, 750 l/s and 500 l/s) for the absorber pumps distributed along the chamber.
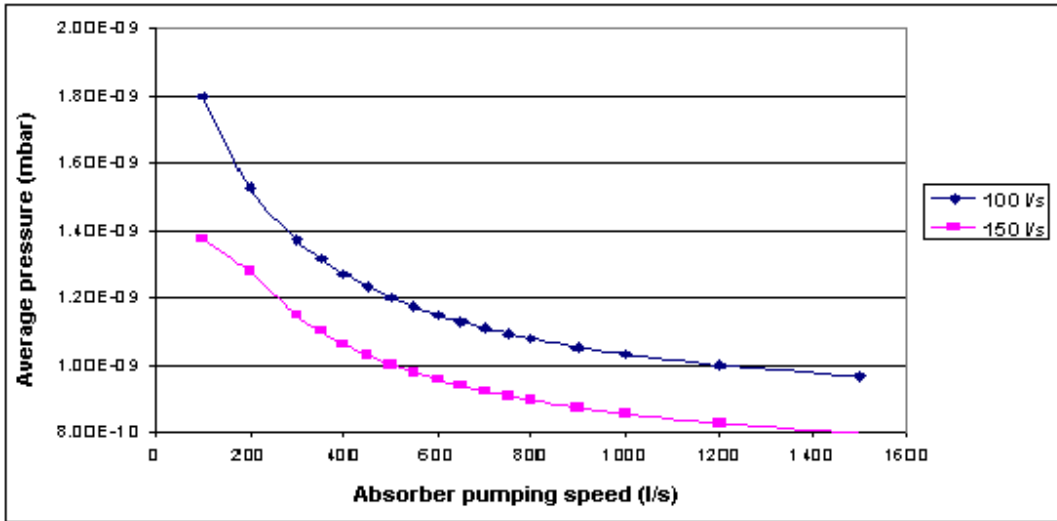
Figure 7.10: Average pressure variation with the absorber pumps pumping speed of 100 l/s and 150 l/s and with the pumps distributed along the chamber
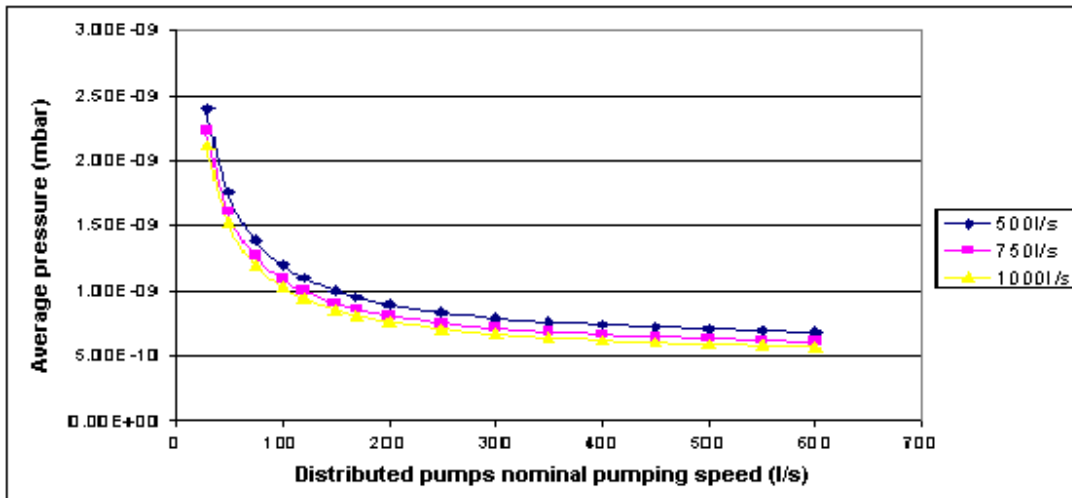
Figure 7.11: Average pressure variation with different pumping speeds, the absorber pumps are distributed along the chamber

Figures (7.10) and (7.11) are for a system with two absorbers (200mm width) and pumps along the vacuum chamber with 100mm width. The figures could be used to optimize the pumping speed required for such a system. With absorbers effective pumping speed selected to be 500l/s, pumps distributed along the vacuum chamber would be preferred to have pumping speed of 100-200 l/s, because below 100 l/s the pressure value is not satisfactory, and over 200 the value of the pressure has only small variations due to conductance limitation.

85

A proposal for the pumps pumping speed for SESAME could be made to have for the absorbers an effective pumping speed of 750 l/s and for the pumps distributed along the storage ring an effective pumping speed not less than 100 l/s.

Increasing the pumping speed may help getting better vacuum but some improvements in the design may also give the same results; in general, increasing the area of port's aperture (the width and the gap) will increase the transmission probability (and so increasing the effective pumping speed of the pumps), also opening out the spouts (wider profile up to the pump) will increase the effective pumping speed (e.g. by a factor of two for nominal pumping speed of 500 l/s). Installation of the pumping port underneath the vacuum chamber with short pumping port may also help having better effective pumping speed.

It is important to mention that in the estimated pressure profiles, synchrotron from the dipoles was only considered and further calculations need to be done to consider the synchrotron radiation from the insertion devices. Also it is worth mentioning that the calculated pressure values are just estimations of the pressure values in the chamber, and the real values might be a little different. So in order to be on the safe side, it is better to have an arrangement of the pumps that gives the lowest value for the pressure.

7.6 Lumped or Distributed Pumping?

The decision of having lumped or distributed pumps along the vacuum chamber depends on many factors; gas load, pressure profile, vacuum chamber profile, conditioning time, in-situ bake out, engineering requirements, space available, cost…etc.

In general for a gas molecule to be removed by the vacuum system, it has to find its way into the pump and be trapped. Thus the rate at which gas can be removed from the system (i.e. the pumping speed) is determined by the product of the arrival rate of the gas molecules at the pump and the capture coefficient of the pump for such molecules.

If the capture coefficient is close to 1, then the only way to decrease the pressure is by increasing the arrival rate.

For a lumped pump, the area of the pump entrance aperture and the transmission of the molecules determine the arrival rate through the pump throat to the pump body.

For a distributed pump, only the area presented by the pump to the molecules determines the arrival rate.

Lumped pumps are cheaper compared to the distributed pumps since they are of standard ranges available in the market, while the distributed pumps are designed on request, which makes them more expensive. The installation and maintenance of the lumped pumps could be easier compared to the distributed pumps, because the installation and maintenance of the distributed pumps may require removal of the major vacuum vessels. It should also be noted that the lumped pumps could be separated easily from the system by using valves, which is not possible with the distributed pumps.

Since the pressure profiles show clearly that lumped pumping of the system is sufficient to achieve a pressure of 1.23×10^{-9} mbar, without considering any improvements, lumped pumping is a good proposal for the vacuum system. Once the synchrotron radiation of the insertion devices was included in the calculations, if places with high gas load (high pressure) originate, then distributed pumps could be used (just in case the lumped pumps close to these areas couldn't solve the problem).

To increase the transmission probability of the system, a proposal for the lumped pumping can be made by allowing the pumping spout to be short, wide and as close to the vacuum chamber as possible; installation of the pumping port underneath the vacuum chamber will give all of these [8].

7.7 Pumps Selection

7.7.1 Rough Pumping

Rough pumping is required so as to achieve pressure below 10^{-6} mbar so that the UHV pumps can be started. The time required to achieve such pressure is important during the conditioning stage. The volume of the system and the gas flow conductance are the main factors in the evaluation of the pumping down of the system.

It would be a good decision to use turbo molecular pump because of its good performance (turbo molecular pumps are clean if magnetic bearings have been used, and provide pressure down to 10^{-6} mbar). Taking the high cost of the turbo molecular pumps into consideration, and also the requirements for another rough pump to reach high vacuum so that the turbo pump can operate, it is better to have a station for the one quarter of the ring, if the calculations gave a short pumping time for single station for two cells of the ring.

Scroll pumps are good candidates to be used with the turbo molecular pump to achieve pressure 10^{-2} mbar; they are cheap, light and clean [9].

7.7.2 UHV Pumps

In General, Ion pumps and gutter pumps are used in the storage rings.

The ion pumps could be of several types: the Diode ion pump, the Noble Diode ion pump, and the Triode ion pump.

The diode ion pump has a pumping speed twice higher than that of the triode pump at 10^{-9} mbar for all reactive gases; CO, CO_2, H_2. The pumping speed for noble gases is approximately 5% less than that of the quoted pumping speed for N_2. Also the further pumping liberates the previously buried noble gas molecules and results in unstable pumping behavior 'instability of the noble gases'. Using Triode pumps reduces the instability of the noble gases, and the pumping speed for the noble gases increases by 15% approximately. The Noble Diode pump utilizes a Tantalum cathode in place of the Titanium cathode of the Diode pump, which increases pumping speed and stability for noble gases.

The NEG and titanium sublimation pumps have a considerable pumping speed for hydrogen and all reactive gases, but do not pump noble gases and hydrocarbons. Also the pumping material requires periodic regeneration to maintain pumping performance, by heating to 400°C approximately.

Diode Ion pump is a good proposal and is sufficient to pump down the storage ring to the required pressure. Using noble diode ion pump is effective in pumping the noble gases, and for high pressure locations where a large pumping speed is required, NEG or TSP will solve the problem. [10], [11]

7.8 Vacuum Instrumentation

The measurement of vacuum is as much important as providing the required vacuum. The total and partial pressure must be correctly measured. Locations of the gauge heads throughout the facility need to be determined, and the specifications and the types of gauges must be studied carefully.

7.8.1 Total Pressure Gauges

It is necessary to measure total pressures down to UHV (i.e. $< 10^{-9}$ mbar) throughout the vacuum system and the gauge system is needed to do this. The storage ring and the beam port front ends require reliable readings of total pressure at 1×10^{-10} mbar. The injector pressure measurement system requires a reliable reading down to 1×10^{-9} mbar.

Unfortunately, it is not possible to cover the whole pressure range with a single gauge; a first gauge is required to cover low and medium vacuum (from atm. to 10^{-3} mbar) and that will also be

useful to provide reading during pumping down the system and during vacuum failure. A second gauge is required for UHV readings as well.

For low and medium vacuum ranges, since the reading is just required to give an indication of the situation, there is no need to use a very accurate gauge, so a gauge such as Pirani gauge is a good choice, and it covers the range from atm. to 10^{-3} mbar.

For the UHV range, two types of gauges are in common use on the accelerators around the world: cold cathode gauges and hot cathode gauges.

The hot cathode gauge needs a third gauge to cover readings between 10^{-3} and 5×10^{-4} mbar. Also penning discharge cold cathode gauge does not cover values below 10^{-9} mbar, while inverted magnetron discharge cold cathode gauge covers pressure ranges from 10^{-3} down to 10^{-11} mbar. For the injector, penning gauge could be used as long as pressure is below 10^{-9} mbar.

Each part of the accelerator must be covered by a pressure gauge. In general, each vacuum section (area between two gate valves) should contain one pair of total pressure gauges, and may require another gauge in case of failure of the first pair. Also the RF cavity, injection straight section, injector vacuum system, rough pump set, all should have at least one pair of total pressure gauges.

Interlock provision needs to be provided to switch on/off the ion pumps, rough pumps, valves, operation of other gauges and RGAs [12].

7.8.2 Partial Pressure Gauges:

It is important for UHV applications to know the composition of the residual gases within the system. Quadrupole mass spectrometer used as Residual Gas Analyzer (RGA) measures the partial pressure of the gases in the system.

The RGA should give full coverage for the vacuum sections and close to the crotch absorbers. So it is required to locate them close to the down stream of the dipole magnets. At least one RGA is needed for each part of the accelerator; the injector vacuum system, the injection straight section, the RF cavity and the ID straight section.

Control units of all the gauges and the other vacuum equipments need to be provided with all necessary cables, interlocks, front panels… etc, and they should have the ability to influence the main control system.

Figure (7.12) shows a vacuum flow diagram for one cell of SESAME. This diagram shows the locations of the pumps gauges and the valves. These locations are optimized to have better vacuum performance.
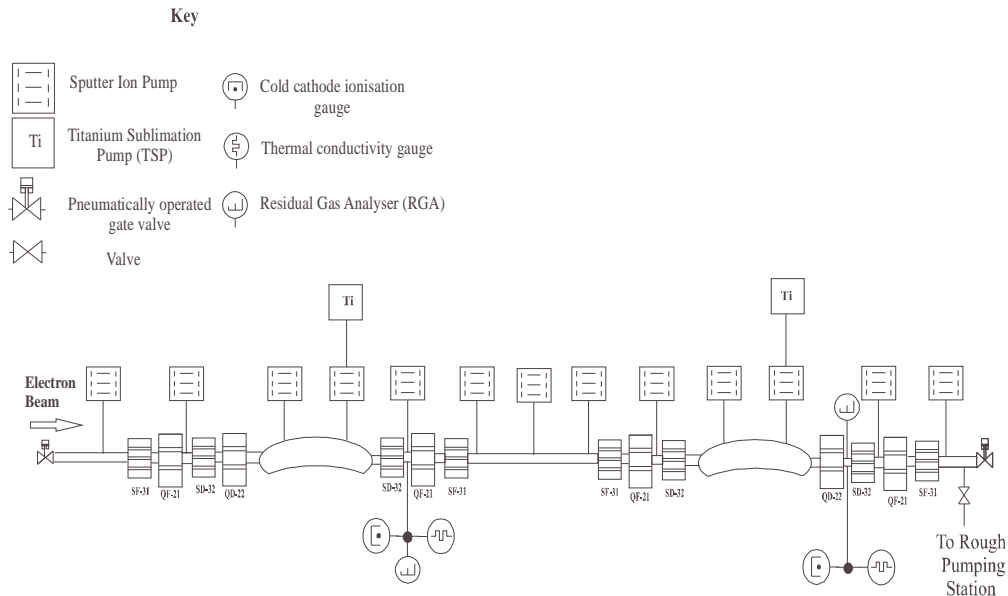
Figure 7.12: SESAME vacuum flow diagram (gauges, pumps and valves types and locations)

7.9 In-sit Bake Out

The in-situ bake out is mainly required in the early stages of a vacuum cycle, see Figure (7.4). After beam scrubbing of 100A.h the results for in-situ bake out and not an in-situ bake out are just the same for the lifetime of the beam. Also the thickness of the heater and the insulation leads to larger magnets which directly affect the cost of the magnets. Also there are the cost of the in-situ bake out system (heaters and insulation...) and other accelerator components.

Sufficient cleaning procedure and vacuum firing (900°C) under vacuum (10^{-5} Torr) and pre bake out of the vacuum chamber improve the life time by decreasing the thermal desorption and therefore the base pressure.

So for this stage of the machine design it is proposed not to have an in-situ bake out.

References:

[1]   D. Einfeld, SESAME, "*First Draft of the Conceptional Design, version 8*", March 2002.
[2]   Ron Ried, "*Materials choice for Diamond Vacuum System*", (Internal Report) Oct. 2000.
[3]   Erhard Huttel, "*Materials for Accelerator Vacuum System*".
[4]   Lother Schulz, "*Stainless Steel Vacuum Chambers*" Oct. 2001.
[5]   Shulz et al. *Vacuum System for the Swiss Light Source*"
[6]   D. Lowe, "*CLS Storage Ring Vacuum Chambers*", March 2001.
[7]   Oleg Malyshev et al. "*Calculated Pressure profile Along the Diamond Storage Ring Cell.*" (Internal Report) Jan 2002.
[8]   Ron Reid, "*Lumped or Distributed Pumping?*" (Vacuum Design Notes) Apr. 1996.
[9]   Keith Middleman et al. "*Rough Pumping Systems for Diamond Storage Ring, Part 1 and Part 2*", (Internal Report) Oct. 2001.
[10] E. Huttel, "*The Vacuum System for the Synchrotron Radiation Source ANKA*"
[11] Tom Weston, "*Capture pumps*", Vacuum Design Notes, Feb. 1996.
[12] Joe Herbert, "*Vacuum Instrumentation for Diamond*", (Internal Report) Jan 2002.